Enzyme Engineering
ISSN: 2329-6674
OPEN ACCESS Freely available online
Research Article

Preliminary Exploration of Structure-Function Crosstalk in Colorectal Cancer Research: Protein Structuromics

Ogori A Friday*, Abu J Oneh, Hwa Dai, Na-Sheng Lin

Department of Food Science and Human Nutrition, University of Illinois, Urbana-Champaign, Urbana, IL, 61801, USA

ABSTRACT

Colorectal Cancer (CRC) refers to cancer that develops from the colon or rectum (parts of the large intestine). Signs and symptoms include blood in the stool, changes in bowel movements, weight loss, and fatigue. Since 1923, when the disease was first named, survival rates have always been unsatisfactory. Despite great advances in molecular biology and traditional treatment methods, many questions remain to be answered regarding cancer occurrence and the underlying mechanism. Medical doctors remain stymied regarding tumor recurrence and worsening disease after effective treatment. To better understand the relevant questions, in this study, 20 oncogenes and 20 anti-oncogenes were examined in relation to protein structure, from protein structure analysis and dynamic analysis methods to 3D structure analysis and systematic analysis of the structure–function relationships of proteins. We hope that these analyses will help promote mechanistic research and the development of new treatments for CRC.

Keywords: Colorectal cancer; Protein structure; Protein folding rate; Protein folding trend; Protein secondary structure

INTRODUCTION

Colon and rectal cancer, also known as Colorectal Cancer (CRC), arises from the cells lining the colon or rectum. It is the third most common cancer worldwide and the second leading cause of cancer-related deaths. It often begins as a noncancerous growth, called a polyp, on the inner lining of the colon or rectum and can take several years to develop into cancer [1]. The terms "colon cancer" and "rectal cancer" were first coined by Dr. W. Ernest Miles in 1923. Dr. Miles was a British surgeon who specialized in the treatment of CRC and was among the pioneers in developing surgical techniques to treat the disease [2]. According to the American Cancer Society, the 5-year survival rates for CRC are as follows: localized cancer: 91%, regional cancer: 72%, distant cancer: 14% and all stages combined: 64%. The death rate of CRC has been decreasing over the past few decades due to early detection and improved treatments. In the United States, the age-adjusted death rate for CRC was 14.2 per 100,000 people in 2020 [3].

To understand the mechanism and help develop the best treatment, in addition to focusing on gene mutations [4] or biomarkers [5], increasing research on prion proteins [6] indicates that protein structure-function interactions are critical for life science research, such as the elucidation of disease- or plant-related mechanisms [7]. NMR and Cryo-EM techniques have greatly facilitated such research, further elucidating the interactions [8,9].

Cancer genes fall into two groups: unfavorable prognostic genes and favorable prognostic genes. Relatively high expression levels of unfavorable prognostic genes at diagnosis indicate significantly lower overall survival for the patients. We prefer to call them oncogenes. Relatively high expression levels of favorable prognostic genes at diagnosis are associated with significantly higher overall survival for patients. We call them anti-oncogenes.

The relationship between oncogenes and anti-oncogenes plays a critical role in the development of cancer. Oncogenes promote the development of cancer by stimulating uncontrolled cell growth, while anti-oncogenes help regulate cell growth and prevent the development of cancer. We are interested in the roles of oncogenes and anti-oncogenes in the development of cancer and how targeted therapies can be developed based on the understanding of these genes [10].

Our group has examined 20 oncogenes and 20 anti-oncogenes. First, we analyzed the protein structure in the two groups of proteins in terms of the full length, α-helix length, and β-strand length and examined how these two types of secondary structures contributed to the full protein or sections thereof in terms of length percentage.

Correspondence to: Ogori A Friday, Department of Food Science and Human Nutrition, University of Illinois, Urbana-Champaign, Urbana, IL, 61801, USA, Email: xn8008@hotmail.com

Received: 24-Mar-2023, Manuscript No. EEG-23-22331; **Editor assigned:** 27-Mar-2023, Pre QC No. EEG-23-22331 (PQ); **Reviewed:** 10-Apr-2023, QC No. EEG-23-22331; **Revised:** 17-Apr-2023, Manuscript No. EEG-23-22331 (R);**Published:** 24-Apr-2023, DOI: 10.35248/2329-6674.23.12.212.

Citation: Friday OA, Oneh AJ, Dai H, Lin N (2023) Preliminary Exploration of Structure–Function Crosstalk in Colorectal Cancer Research: Protein Structuromics. Enz Eng. 12:212

The protein length refers to the number of amino acids in the full-length protein or each type of secondary structure. Then molecular dynamics methods were used to determine the protein folding rate, folding trends at different stages, and protein chirality. We gave the research name protein-structromics. We hope that these analyses will help provide new ideas for cancer mechanism research and the development of new treatments.

MATERIALS AND METHODS

Information collection for the two groups of proteins

Twenty genes were selected from each group, suitable proteins without isoforms or variant types were found, and protein information was collected [11].

Protein secondary structure prediction

We followed the Kelley methods for prediction [12].

Protein folding rate prediction

The Gromiha methods for testing were used to consider protein characteristics and separate all α-helix and mixed types [13-16].

Protein folding trend prediction

We followed the Grau l and Joel Roca-Martinez methods [17,18].

Protein 3D folding

The best structures were chosen with assistance from AlphaFold [19].

Basic protein information collection

Suitable protein GenBank IDs were selected and listed, and the number of amino acids was collected as the protein length. With the sequence information, we analyzed and obtained the folding rate and the full length, α-helix length, and β-strand length of the whole sequence, each as the arithmetic mean [11].

Moreover, we calculated the α-helix sectional length, α-helix% sectional length, β-strand sectional length, and β-strand% sectional length.

Whole protein sequence and sectional sequence analysis

First, we analyzed the full length of each of the two groups, performed internal and between-group comparisons of the whole α-helix length and β-strand length, α-helix sectional length, and β-strand sectional length, and separated the full- length proteins into four parts, each 1/4 of the whole length (Figure 1). The normality test for each part showed that nearly every table has some results with skewed distributions. Then, a nonparametric test was performed, and the threshold for significant differences was $p<0.05$. We found that the average full length of the favorable group was significantly greater than that of the unfavorable group (Table 1). For the full-length structures, internal comparison of the secondary structures of the two groups showed that in both groups, the α-helix length was significantly longer than the β-strand length; cross comparison showed that the favorable group had a significantly longer average β-strand length than the unfavorable group, while the amount of α-helix in the two groups showed no significant difference (Table 2).

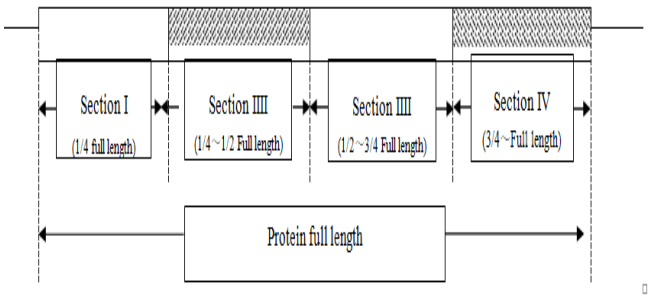

Figure 1: Whole protein length separate principle.

Table 1: Two group lengths compare with non-parametric test.

Group	Unfavorable	Favorable
n	20	20
Mean	498.65	649.35
Std. Deviation	297	284.46
P value	0.035	

Table 2: Two groups contend length compare with non-parametric test.

Internal group compare (a-helix length vs. b-strand length)		
Group	Unfavorable	Favorable
P value	<0.001	0.005
Two groups cross compare		
Composition	a-helix length	b-strand length
P value	0.478	0.005

RESULTS

In the sectional comparison, we found that the groups did not have significantly different internal averages.

Afterward, we rearranged the order based on increasing protein length. The numbers under the X-axis in Figures 2A and 2B belong to the original sequence in. By analyzing the folding rate trend curves of the proteins in the two figures, we found that as the protein length increased, the protein folding rates in both groups gradually increased, but the favorable group had a higher value than the unfavorable group (Figures 2A and 2B).

Then, we listed the folding rate with the secondary structure sectional length percentage. The curves in the four figures show that the two types of secondary structures in different sections have some effects on the folding rate. Moreover, the figures show that all α-helical proteins and all proteins containing both types of secondary structure showed similar trends. As the folding rate increased, the α-helix% in both groups increased, but the β-strand% decreased (Figures 3A and 3B).

Five trends and 3D structure of proteins

For the two groups of proteins in the early stage, the backbone, side chain, α-helix and β-strand trend dynamic curves and the 3D structures are presented.

Considering the five trends and 3D structures of the two groups of proteins, we separated the protein structures into five kinds: packed, simple, middle, loose, and shaker (Table 3).

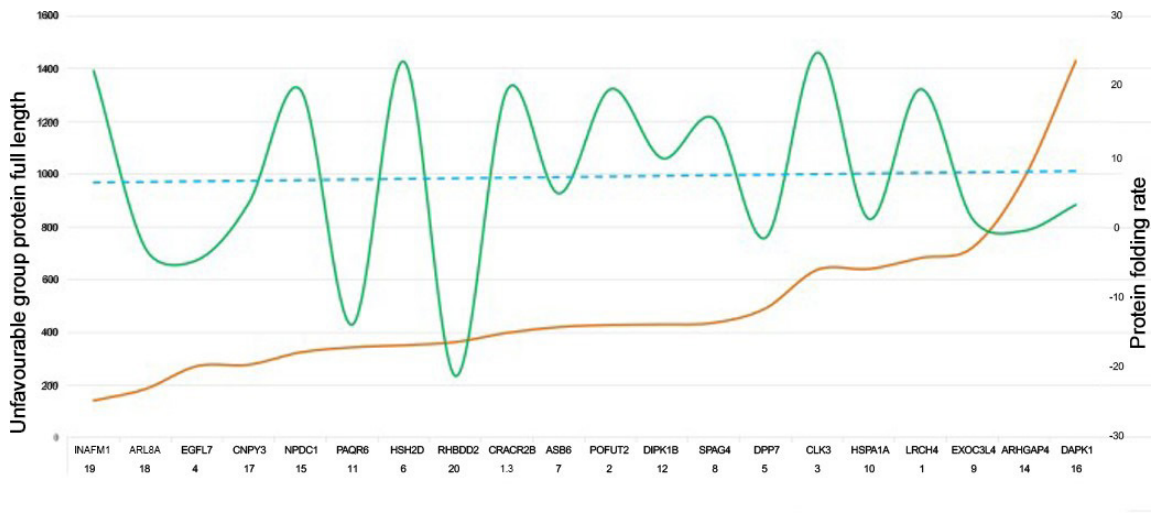

Figure 2A: Proteins full length and protein folding rate relationship. Unfavorable group proteins length increases curve and protein folding rate trends curve. **Note:** (——): Protein full length; (——): Protein folding rate; (——): Protein folding rate trend.

Figure 2B: Proteins full length and protein folding rate relationship. Favorable group proteins length increases curve and protein folding rate trends curve. **Note:** (——): Protein full length; (——): Protein folding rate; (——): Protein folding rate trend.

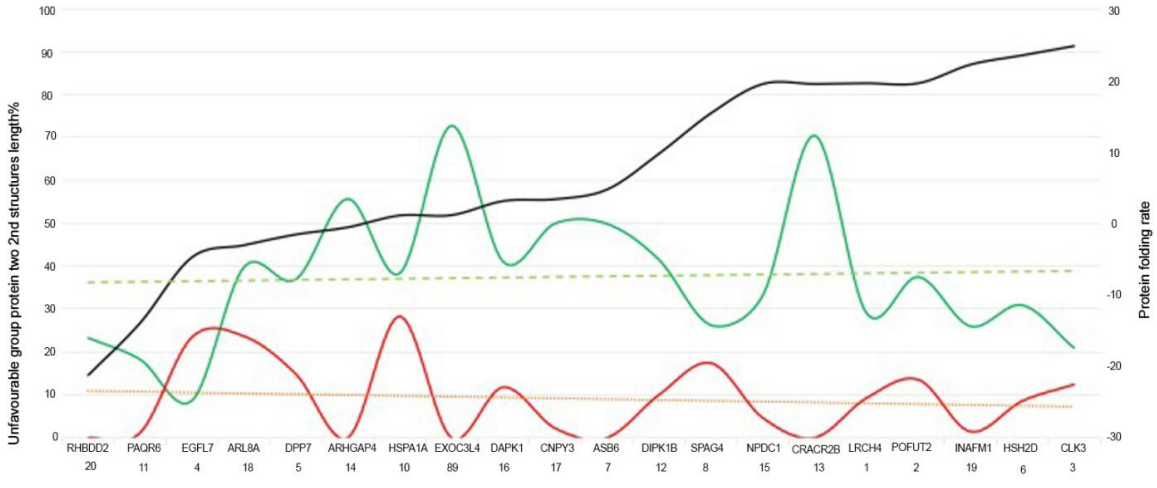

Figure 3A: Protein folding trend and two 2nd structure analyses. Unfavorable group proteins two 2nd structures length increases curve and protein folding rate trends curve. **Note:** (——) a-helix%; (——) b-strand%; (——) Protein folding rate; (——) Helix%trend, (——) Strand% trend.

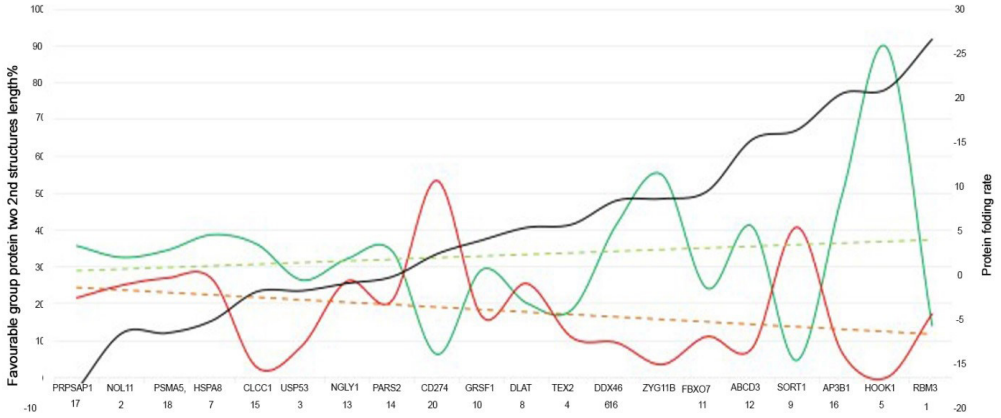

Figure 3B: Protein folding trend and two 2nd structure analyses. Favorable group proteins two 2nd structures length increases curve and protein folding rate trends curve. **Note:** (——) a-helix%; (——) b-strand%; (——) Protein folding rate; (——) Helix%trend, (——) Strand% trend.

Table 3: Protein multi-structure analysis.

Protein classify	Group			
	Unfavorable group		Favorable group	
	Number	Protein name	Number	Protein name
Packet	11	POFUT2, CLK3, DPP7, EXOC3L4, HSPA1A, PAQR6, DIPK1B, ARHGAP4, DAPK1, ARL8A, RHBDD2	9	NOL11, ZYG11B, HSPA8, DLAT, SORT1, ABCD3, NGLY1, PARS2, PRPSAP1
Middle	4	EGFL7, CRACR2B, NPDC1,INAFM1	2	RBM3, HOOK1
Simple	2	HSH2D, SPAG4	2	CLCC1, CD274
Loose	2	LRCH4,ASB6	3	USP53, TEX2,DDX46
Shaker	1	CNPY3	4	FBXO7, AP3B1, PSMA5, GRSF1
Total	20	-	20	-

DISCUSSION

The microenvironment of CRC is complex and involves interactions between cancer cells, immune cells, stromal cells, and the extracellular matrix. One of the key features of this microenvironment is chronic inflammation, which can promote tumor growth and progression. Considering the tumor environment, CRC is a genetically, anatomically, and transcriptionally heterogeneous disease. The prognosis for a CRC patient depends on the stage of the tumor at diagnosis and widely differs accordingly. The Tumor Microenvironment (TME) in CRC is an important factor affecting targeted cancer therapy. The TME has a dynamic composition including various cell types, such as cancer-associated fibroblasts, tumor-associated macrophages, regulatory T cells, and myeloid-derived suppressor cells, as well as extracellular factors that surround cancer cells and have functional and structural roles under physiological and pathological conditions [20].

The process of CRC development displays the roles of oncogenes against anti-oncogenes. David clearly shows the balance and highlights the importance of maintaining balance between these genes in preventing the development of cancer [21]. Considering the complexity of the cancer development mechanism and the need to develop new treatment methods, based on information on the wild-type P53 protein misfolding and cytosolic localization are contributing to its inactivation in myeloid Leukemia [22], this paper focuses on protein multilevel structural characteristics to better understand oncogene and anti-oncogene structural characteristics.

We found that the favorable group had a significantly longer average protein length than the unfavorable group (Table 1) [23]. Therefore, favorable group proteins might have more complex structures and greater stability than unfavorable group proteins. Internal comparison of the lengths of the two types of secondary structure at the whole sequence level showed that the α-helix length was significantly greater than the β-strand length, but cross comparison showed that the favorable group had a greater β-strand length than the unfavorable group, but the two groups had no difference in α-helix lengths. Those differences may affect protein folding. Moreover, we found that no significant differences in the two types of secondary structures at the sectional level. Both types of secondary structure are important for keeping the protein stable. During protein folding, the formation of the α-helix is a key step in the establishment of the protein's tertiary structure. The α-helices can serve as structural elements that help to organize the overall shape of the protein, providing stability and rigidity to the structure. Additionally, α-helices can participate in protein-protein interactions, which are important for many biological processes [24]. The formation of the β-strand is also important for protein folding and helps to stabilize the protein's tertiary structure. The β-strand can also participate in the formation of larger structural elements, such as β-barrels, which are found in many membrane proteins [25]. Comparing the two types of secondary structures and sectional content of the two groups showed that the unfavorable group proteins have a more complex structure, which would make the unfavorable group proteins more stable than the favorable group proteins, promoting cancer development. The protein length and content comparison results seem to be inconsistent.

Therefore, we need more evidence to explain the situation.

Combining protein lengths, percentages of the two types of protein secondary structure, and protein folding rates together, an interesting variety of relationships were revealed: first, according to the arithmetic mean folding rate of the favorable group is faster than that of the unfavorable group; second, the two groups have similar total α-helix lengths, but the favorable group has a longer total β-strand length than the unfavorable group (Table 2); third, considering the relationship between protein length and protein folding rate, as the full length of the proteins increases, the folding rate of the unfavorable group remains steady, but that of the favorable group increases (Figures 2A and 2B); and fourth, when we examined the folding rates and the full-length percentage and sectional percentages of the two types of secondary structure together, the results all indicated that both secondary structure percentages abide by the same principles as the combination of full length and folding rate, as the amount of secondary structure in the unfavorable group show only a small increasing trend with total length, while the favorable group shows an increasing trend (Figures 3A and 3B). All of these results indicate that the analysis results of the protein length, protein content, and protein folding rate in the two groups of proteins were quite complex, and we were unable to reach consistent conclusions. Therefore, we believe that combining dynamic factors with a 3D structure could be greatly helpful in deep data mining.

We obtained statistical folding trends for approximately 40 proteins, including the early stage, final backbones, side chains, α-helix length, and β-strand length, assisted by 3D structures. In a multilevel comparison, all 40 proteins fall into five categories as follows. First, some proteins show peaks in the early stage and backbone trends are evenly distributed over the entire sequence; side chain conformations tend to display two chiralities kept in balance; α-helices and β-strands show uniform structure distributions; and the 3D structures are quite complex, with a central core surrounded by subcore structures or many cores interacting; these proteins also tend to show evenly distributed cis and trans side chain structure. We call these packet proteins. Second, short proteins, most under 100 aa, show a degree of early-stage peak concentration and ultimately show concentrated peaks in parts of the whole sequence. The two kinds of secondary structures show a similar behavior, and the protein may have one or more simple functional cores. The distribution of protein side chains tends toward either cis or trans, which in turn affects the distribution and trends of the two types of secondary structure. We call this kind of protein is simple. Third, some proteins exhibit trends and 3D structure complexity between those of packet and simple proteins, and we have named this type middle. Fourth, Early-stage peaks and backbone trends are clustered at certain positions in the full sequence; the whole protein contains more than one central core structure; backbone trends show some high peaks, while other nearby peaks are lower; and the two types of secondary structure show their highest peaks at the same amino acid site or close together. The central cores are close but not like the packet proteins, and each core remains independent. We call this type of protein loose. Fifth, some proteins have one or more strong core structures, even backbone trend distributions, and balanced side chain chirality; however, the central cores are not protected by subcores but surrounded by small structures or even with random coil. The tertiary structures of such proteins are easily affected by changes in the environment, and we named this type shaker. Because the packet protein has a central core protected by many subcores, the side chains show balanced chiralities, the α-helix and β-strand show uniform structural distributions, and the 3D structures are quite complex, packet-type proteins consistently maintain their function. However, the other four kinds are not protected and easily undergo structural changes in response to changes in environmental factors, such as ions, temperature, and pH. The folding rate of the unfavorable group tended to increase with increasing protein length in Figures 2A and 2B, and the unfavorable group contained more packet proteins than the favorable group (Table 3). Therefore, unfavorable group proteins were better protected than favorable group proteins.

The treatment of CRC depends on several factors, including the stage of the cancer, the location and size of the tumor, and the patient's overall health. Treatment options may include surgery, radiation therapy, chemotherapy, and targeted therapy.

To better understand CRC development, traditional research has focused on protein mutations, such as KRAS, NRAS and BRAF mutations [26], and on DNA or RNA sequencing analysis. We believe that including DNA and RNA mutations, isoform appearance, and variant new versions will contribute to translating genotype into phenotype, and changes in status should be shown after related proteins are activated. In addition to research on the two kinds of nucleic acid, protein structure also needs to be a focus, as diseases can be caused by changes in protein structure that affect the ability of the protein to bind other molecules and carry out its function or by conformational changes that affect protein solubility and degradability. In amyloidosis/AL, immunoglobulin chains form an insoluble protein aggregate called amyloid in organs and tissues [27].

Surgery, radiation, and drugs can change our cell microenvironment. Surgery can alter the human TME, as can radioactivity [28-30]. Drugs can also change the TME, even leading to drug resistance [31,32].

The 40 proteins we examined in colon and rectum cells showed no isoforms and no mutations. While health was maintained, the protein expression of the two groups remained balanced; however, the unfavorable group proteins had a higher folding rate than the favorable group proteins, and the unfavorable group contained more packet-type proteins. Therefore, when tumors occur, the balance is broken, and the unfavorable group retains more functional proteins than the favorable group; at the same time, as disease alters aspects of our cell microenvironment, such as ion concentration and pH, the favorable group proteins lose their functions more easily than the unfavorable group. Interestingly, when we treat patients with surgery, radioactivity, and medicines, these treatments also change our cell microenvironment, which may lead to indiscriminate harm. Initially, treatment seemed to control patient illness and the effects on both groups of proteins damaged by microenvironmental changes, including packet-type proteins. Later, with the changing situation, the more favorable group lost more functions than the unfavorable group, and as shown in Figure 2A, we observed more unfavorable group packet-type protein folding, but the favorable group did not maintain folding as well. At this time, the balance of the two groups was broken again.

CONCLUSION

The patient's condition deteriorated again, and even with more treatments, the microenvironment worsened, depressing the anti-oncogene-related protein function-folding and breaking the ones that remained functional. If we consider isoforms and mutations, the situation may become worse. Therefore, my suggestion is that

in conjunction with treatment methods, we should adjust the microenvironment at the same time and even test the level of activity of favorable proteins, seek to promote the positive balance of the two groups, and support the correct folding of anti-oncogene-related proteins for activation after expression.

ACKNOWLEDGEMENTS

We would like to thank Prof. Licheng Zhao, Dean of Medicine College of Jinzhou Medical University, for supporting us with research equipment. TopEdit English Editing LLC helped us with figure editing as a complimentary service.

COMPETING INTERESTS

The authors declare no competing interests.

AUTHOR CONTRIBUTIONS

Guangshuai Xu, Xingqi Li and Zhibo Chen were responsible for reference collection. Jinhua Yang and Jing Zhang collected gene and reference information. Guang Yang, Chi Li and Kang Liu collected protein secondary structure and dynamic results. Yingxin Li and Chaoqun Yin collected protein 3D structure data; Xin Pan and Zhina Wang were charged with analysis of data and results and related clinical information analysis; and Nan Xiao was charged with data management, results analysis and wrote the paper. Nan Xiao, Jing Zhang, and Guangshuai Xu are co-first authors.

REFERENCES

1. Arnold M, Sierra MS, Laversanne M, Soerjomataram I, Jemal A, Bray F. Global patterns and trends in colorectal cancer incidence and mortality. Gut. 2017;66(4):683-691.
2. Campos FG. The life and legacy of William Ernest Miles (1869-1947): a tribute to an admirable surgeon. Rev Assoc Med Bras. 2013;59:181-185.
3. Siegel RL, Miller KD, Fuchs HE, Jemal A, et al. Cancer statistics, 2021. CA Cancer J Clin. 2021;71(1):7-33.
4. Takehara K, Ishizaki Y, Nagakari K, Ohuchi M, Fukunaga M, Sakamoto K. A Patient with Transverse Colon Cancer Complicated by Cowden Syndrome Administered FOLFOXIRI+ Bevacizumab Therapy. Case Rep Gastroenterol. 2022;17:56-63.
5. Yang Y, Meng WJ, Wang ZQ. MicroRNAs in colon and rectal cancer-novel biomarkers from diagnosis to therapy. Endocr Metab Immune Disord Drug Targets. 2020;20(8):1211-1226.
6. Kovač V, Čurin Šerbec V. Prion protein: the molecule of many forms and faces. Int J Mol Sci. 2022;23(3):1232.
7. Hodge EA, Benhaim MA, Lee KK. Bridging protein structure, dynamics, and function using hydrogen/deuterium-exchange mass spectrometry. Protein Sci. 2020;29(4):843-55.
8. Skeens E, Lisi GP. Analysis of coordinated NMR chemical shifts to map allosteric regulatory networks in proteins. Methods. 2023;209:40-47.
9. Xiao L, Magupalli VG, Wu H. Cryo-EM structures of the active NLRP3 inflammasome disc. Nature. 2023;613(7944):595-600.
10. D'ambrogio A, Nagaoka K, Richter JD. Translational control of cell growth and malignancy by the CPEBs. Nat Rev Cancer. 2013;13(4):283-290.
11. Yang W, Shi J, Zhou Y, Liu T, Zhan F, Zhang K, et al. Integrating proteomics and transcriptomics for the identification of potential targets in early colorectal cancer. Int J Oncol. 2019;55(2):439-450.
12. Kelley LA, Mezulis S, Yates CM, Wass MN, Sternberg MJ. The Phyre2 web portal for protein modeling, prediction and analysis. Nat Protoc. 2015;10(6):845-858.
13. Gromiha MM, Selvaraj S. Comparison between long-range interactions and contact order in determining the folding rate of two-state proteins: application of long-range order to folding rate prediction. J Mol Biol. 2001;310(1):27-32.
14. Gromiha MM. Importance of native-state topology for determining the folding rate of two-state proteins. J Chem Inf Comput Sci. 2003;43(5):1481-5.
15. Gromiha MM. A statistical model for predicting protein folding rates from amino acid sequence with structural class information. J Chem Inf Model. 2005;45(2):494-501.
16. Gromiha MM, Thangakani AM, Selvaraj S. FOLD-RATE: prediction of protein folding rates from amino acid sequence. Nucleic Acids Res. 2006;34:70-74.
17. Grau I, Nowé A, Vranken W. Interpreting a black box predictor to gain insights into early folding mechanisms. Comput Struct Biotechnol J. 2021;19:4919-4930.
18. Roca-Martinez J, Lazar T, Gavalda-Garcia J, Bickel D, Pancsa R, Dixit B, et al. Challenges in describing the conformation and dynamics of proteins with ambiguous behavior. Front Mol Biosci. 2022;9.
19. Varadi M, Anyango S, Deshpande M, Nair S, Natassia C, Yordanova G, et al. AlphaFold Protein Structure Database: massively expanding the structural coverage of protein-sequence space with high-accuracy models. Nucleic Acids Res. 2022;50:D439-44.
20. Gallo G, Vescio G, De Paola G, Sammarco G. Therapeutic targets and tumor microenvironment in colorectal cancer. J Clin Med. 2021;10(11):2295.
21. Hoyos D, Zappasodi R, Schulze I, Sethna Z, de Andrade KC, Bajorin DF, et al. Fundamental immune–oncogenicity trade-offs define driver mutation fitness. Nature. 2022;606(7912):172-179.
22. Eckstein OS, Wang L, Punia JN, Kornblau SM, Andreeff M, Wheeler DA, et al. Mixed-phenotype acute leukemia (MPAL) exhibits frequent mutations in DNMT3A and activated signaling genes. Exp Hematol. 2016;44(8):740-744.
23. Brocchieri L, Karlin S. Protein length in eukaryotic and prokaryotic proteomes. Nucleic Acids Res. 2005;33(10):3390-3400.
24. Khorasanizadeh S, Peters ID, Roder H. Evidence for a three-state model of protein folding from kinetic analysis of ubiquitin variants with altered core residues. Nat Struct Biol. 1996;3(2):193-205.
25. Plaxco KW, Simons KT, Baker D. Contact order, transition state placement and the refolding rates of single domain proteins. J Mol Biol. 1998;277(4):985-994.
26. Bożyk A, Krawczyk P, Reszka K, Krukowska K, Kolak A, Mańdziuk S, et al. Correlation between KRAS, NRAS and BRAF mutations and tumor localizations in patients with primary and metastatic colorectal cancer. Arch Med Sci. 2022;18(5):1221.
27. Fändrich M, Schmidt M. Methods to study the structure of misfolded protein states in systemic amyloidosis. Biochem Soc Trans. 2021;49(2):977-985.
28. Cheng X, Zhang H, Hamad A, Huang H, Tsung A. Surgery-mediated tumor-promoting effects on the immune microenvironment. Semin Cancer Biol. 2022; 86:408-419.
29. Iesato A, Nucera C. Tumor Microenvironment–Associated Pericyte Populations May Impact Therapeutic Response in Thyroid Cancer. Adv Exp Med Biol. 2021;1329:253-269.
30. Castillo-Rivera F, Ondo-Méndez A, Guglielmi J, Guigonis JM, Jing L, Lindenthal S, et al. Tumor microenvironment affects exogenous sodium/iodide symporter expression. Transl Oncol. 2021;14(1):100937.

31. Junttila MR, De Sauvage FJ. Influence of tumour micro-environment heterogeneity on therapeutic response. Nature. 2013;501(7467):346-354.

32. Zhang W, Ke Y, Liu X, Jin M, Huang G. Drug resistance in NSCLC is associated with tumor micro-environment. Reprod Biol. 2022;22(3):100680.